Cloud-type analysis of Himawari-8 meteorological satellite data with ancillary data from ground-based instruments

Takashi Kadowaki, Nofel Lagrosas, and Hiroaki Kuze

Center for Environmental Remote Sensing, Chiba University, Chiba, Japan
Email:kadowaki1005@chiba-u.jp; nofel@chiba-u.jp; hkuze@faculty.chiba-u.jp

KEY WORDS: Himawari-8, Cloud coverage, Cloud classification, CALIPSO, Aerosol

ABSTRACT: Clouds control the radiation balance and water circulation in the atmosphere, and hence, the characterization of clouds and their behavior is one of the important tasks for both satellite and ground-based remote sensing. In the present study, we retrieve cloud physical (e.g., cloud types, cloud coverage and phase) and optical (e.g., opacity) information by employing Himawari-8 meteorological satellite data over the Japan area. The cloud coverage information is obtained from bands 1, 6, 8, 9, 13, 14, 15 and 16 of the Himawari-8 AHI (Advanced Himawari Imager) sensor. The cloud altitudes are retrieved from CALIPSO (Cloud Aerosol Lidar and Infrared Pathfinder Satellite Observation) data, while the concurrent data of aerosol are obtained from the ground-based instruments, namely, a sunphotometer, an integrated nephelometer, and an aethalometer. The sunphotometer measures aerosol optical thickness at wavelengths of 450, 550, and 770 nm. CALIPSO data provide the vertical distribution of aerosols and clouds as well as that of cloud phase when it passes over Chiba. We apply the split window algorithm (SWA) to classify clouds into nine different types. We compare the resulting cloud types with results based on the HCAI (High Resolution Cloud Analysis Information) algorithm developed by the Japan Meteorological Agency. The comparison indicates that good agreements are found for cirrus, whereas some differences are seen for cumulonimbus and middle cloud underneath dense cirrus regions. As a whole, the implementation of these methods on datasets derived from long-term observation can offer climatological trends of cloud occurrence over different areas in Japan.

1. Introduction

Climate change due to the anthropogenic emission of greenhouse gases exerts various effects in the Earth's environment (Rajendra, 2014). In recent years, the frequent occurrence of heavy rain events causes severe damages worldwide. Since clouds are one of the essential factors that control precipitation, it is vitally important to investigate the characteristics of clouds using various datasets from both satellite and ground-based observations (Stefanie, 2016). Himawari-8 was launched in October 2014 as a first satellite that belong to a series of third generation, geostationary meteorological satellites. The sensor, advanced Himawari imager (AHI), provides data from 16 bands including three visible (VIS), one near-infrared (NIR), two short-wave infrared (SWIR), and ten thermal infrared (TIR) bands. The full disk image is recorded every 10 min, and the Japan area is covered in every 2.5 min (Murata, 2016). Table 1 shows information for each observation band, number of pixels and spatial resolution of Himawari-8 (Higuchi, 2018).

In this study, we employ gridded data of Himawari-8 global-scan, full-disk image provided from the Center for Environmental Remote Sensing (CEReS) for cloud detection and classification in the Japan area (Higuchi, 2018). The range used for the analysis is 85° to 205° east longitude and 60° north latitude to 60° south latitude. For implementing cloud classification, here we employ two different algorithms of the high-resolution cloud analysis information (HCAI) and split-window algorithm (SWA). The first algorithm, HCAI, was proposed by Japan Meteorological Agency as a method for creating a basic cloud product consisting of cloud top altitude, cloud phase information, and cloud phase (Suzuki, 2018). The classification scheme of HCAI is based on the fractional/homogeneous features as well as opaque/transparent appearance of cloud systems. In the case of SWA, on the other hand, the discrimination of the cloud types is made on the basis of the threshold values of brightness temperature (BT) and BT difference among TIR bands. In a recently proposed form of SWA, the combination of band 13 (10.4 □m) and band 15 (12.4 □m) has been used to classify clouds into nine different types around the Japan area (Purbantoro et al., 2018).

In addition to the Himawari-8 data, we exploit the space lidar data of CALIPSO (Cloud Aerosol Lidar and Infrared Pathfinder Satellite Observation) (Charles, 2019) for obtaining the altitude information on the cloud top. Also, the aerosol data from the ground-based instruments are used to discriminate thin clouds and aerosol layers.

Table 1. Himawari-8 gridded data

Gridded data		Himawari-8 band	Pixel*line	Spatial resolution	HCAI	SWA
EXT	01	Band 03 (0.64 μm)	24000*24000	0.005 degree		
VIS	01	Band 01 (0.47 μm)	12000*12000	0.01 degree	○	○
	02	Band 02 (0.51 μm)				
VIS+NIR	03	Band 04 (0.86 μm)				
SIR	01	Band 05 (1.6 μm)	6000*6000	0.02 degree		
	02	Band 06 (2.3 μm)				
TIR	01	Band 13 (10.4 μm)	6000*6000	0.02 degree	○	○
	02	Band 14 (11.2 μm)			○	
	03	Band 15 (12.4 μm)			○	○
	04	Band 16 (13.3 μm)				○
	05	Band 07 (3.9 μm)				
	06	Band 08 (6.2 μm)			○	
	07	Band 09 (6.9 μm)				
	08	Band 10 (7.3 μm)			○	
	09	Band 11 (8.6 μm)			○	
	10	Band 12 (9.6 μm)				

2. Methodology

2.1 HCAI

The Japan Meteorological Agency has proposed the HCAI algorithm as a method for creating a basic cloud product consisting of cloud top altitude, cloud phase information, and cloud phase. Figure 1 shows the procedure of HCAI method (Suzuki, 2018). First, in the detection of cloud regions, the threshold from albedo values from the BT of band 01 (BT01) is set to 0.3, and pixels with albedo values greater and less than 0.3 are classified as cloud and clear areas, respectively. Second, the cloud top altitude is calculated using the monthly lapse rate, and classified into three types: very high / high (7-13 km), middle (2-7 km), and low / very low / extremely low (surface-2 km). Third, as shown in Figure 2, the cloud opacity information is calculated and classified into three types: fractional cloud, opaque cloud, and semi-transparent cloud (Mouri, 2016). At this time, the offset is set based on the specified time, and is classified based on the BTD between band 14 -15 and that between band 11-14.

Clouds classified as opaque are further classified into two types, dense cloud and cumulonimbus, using the BTD between band 10 - 08. Clouds classified as low, very low and extremely low are classified into three different types of cumulous, stratocumulus and stratus/fog by comparing the BT of band 13 with the set threshold value.

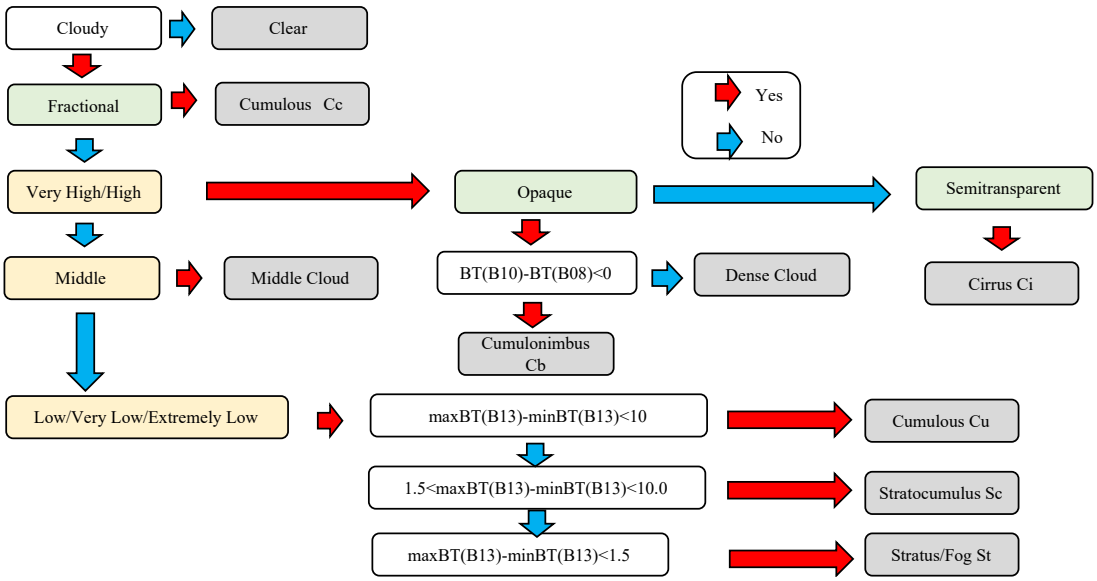

Figure 1 Procedure of HCAI analysis (Suzuki, 2018).

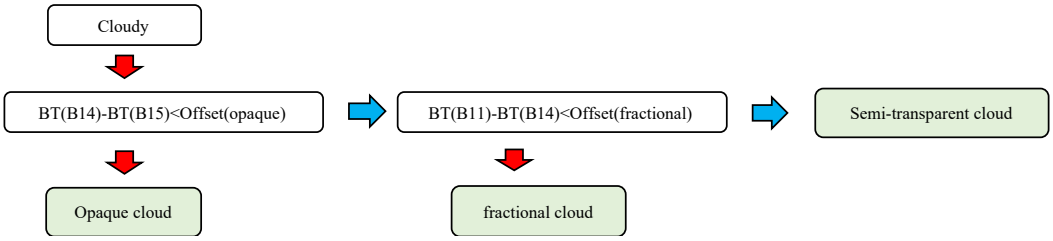

Figure 2 Discrimination of cloud opacity (Suzuki, 2018).

2.2 SWA

In this study, clouds are classified into nine types by means of the split window algorithm (SWA) method (Purbantoro et. al, 2018) and the results are compared with those from HCAI. The nine types are as follows: thick cirrus, cirrus, thin cirrus, dense cirrus, ice cloud, water cloud/stratocumulus/stratus, high cumulonimbus, middle cumulonimbus and cumulus (Figure 3). The discrimination is made with the threshold values of BT and BTD (Table 2), based on the band combinations of band 13 - 15 and band 15 -16 (Purbantoro et al., 2018). The SWA method in Figure 3 shows cloud phase information on the vertical axis and cloud height information on the horizontal axis.

Table 2 Threshold of SWA analysis

	Winter Season		Summer Season	
	SWA13-15	SWA15-16	SWA13-15	SWA15-16
BT-1	245	248	250	253
BT-2	253	256	258	261
BTD-1	0.6	1.0	0.9	0.8
BTD-2	3.2	14	4.5	14

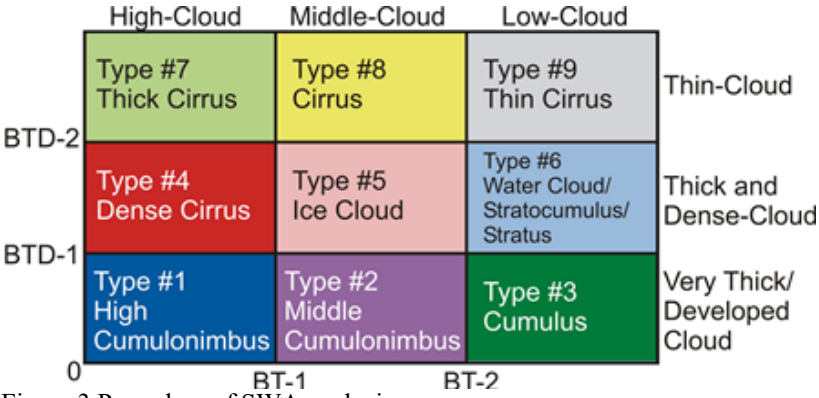

Figure 3 Procedure of SWA analysis

2.3 CALIPSO

CALIPSO is a satellite developed by National Aeronautics and Space Administration (NASA) and European Space Agency (ESA) (Charles, 2019). For observing clouds and aerosols, it is equipped with Cloud-Aerosol Lidar with Orthogonal Polarization (CALIOP), Imaging Infrared Radiometer (IIR), and Wide-Field Camera (WFC). In this study, CALIPSO lidar are downloaded from NASA's website (https://www-calipso.larc.nasa.gov/products/) and compared with the results obtained using HCAI and SWA methods.

2.4 Ground-based instruments

The sunphotometer (Prede, PSF100) is a device that automatically tracks the sun and spectroscopically measures the intensity of direct sunlight at 368, 500, 675 and 778 nm, giving the value of aerosol optical thickness (AOT). In addition, the Angstrom parameter representing the particle distribution can be derived by calibrating and analyzing the signals using the Langley method. The nephelometer (TSI3563) is a sampling instrument that measures the aerosol scattering coefficient at 450, 550, and 700 nm. Similarly the aethalometer (Magee, AE31) measures the aerosol absorption coefficients at seven wavelengths of 370, 450, 570, 615, 660, 880 and 950 nm. The extinction coefficient $\alpha_{ext}(\lambda)$ is the sum of the absorption coefficient $\alpha_{abs}(\lambda)$ obtained from the aethalometer and the scattering coefficient $\alpha_{sca}(\lambda)$ from the nephelometer. We also utilize the visibility value from a visibility-meter (Vaisala, PWD52), which reports the horizontal visibility at 550 nm every 10 min. The value of AOT at each wavelength can be determined also from SKYNET skyradiometers. The values of extinction coefficient, AOT, and visibility are used to evaluate the aerosol loading in the lower atmosphere. In this study, the temporal variation of signals of the sunphotometer and skyradiometer are employed to examine the cloud cover over the CEReS site.

3. Results and discussion

Figure 6 shows the cloud-type distribution retrieved from the Himawari-8 data observed at 03:40 UTC on July 2, 2016. Figure 6(a) and (b) show the results with different band combinations of (a) band 13-15 and (b) band 15-16, while Figure 6(d) that of HCAI. Figure 6(c) shows the color bars corresponding to the types of clouds in the SWA method and the HCAI method. In each panel, the white line indicates the satellite orbit track of CALIPSO. Figures 6(d) and (e) show the cloud component and altitude information observed in the concurrent CALIPSO data. Figure 7 shows the temporal change of the intensity of direct solar radiation observed by the sunphotometer, and Figure 8 shows the AOT observed from sky radiometer.

In the case of Figure 6(a), most of the clouds (38-45° N) within the CALIPSO orbit is type 4 (dense cirrus), while the low-right portion (35-37° N) indicating type 7 (thick cirrus). In Figure 6(b), the upper-left area (42-45° N) indicates type 1 (High cumulonimbus), the middle area (38-42° N) indicates type 4 (dense cirrus), the lower-right area (36-38° N) indicates type 6 (water cloud), and the more lower-right area (35° N) indicates type 9 (thin cirrus). In the case of HCAI shown in Figure 6(c), on the other hand, most of clouds along the CALIPSO track are of type 4 (cirrus) and type 2 (dense cloud), while the lower-right area (36° N) indicating type 5 (middle cloud) and the more lower-right area (36° N) indicating type 7 (stratocumulus).

In the time-height indication of CALIPSO data shown in Figures 6(d) and (e), thick clouds with ice phase are observed in the altitude range of 10-15 km (35-37° N and 40-45° N). Middle and lower layers of water clouds are observed between 5 and 10 km (37-39° N) and 0 and 2 km (35-36° N), respectively. In the case of Figure 6(e), the thick clouds with ice phase observed at 35-37° N and 40-45° N are likely to be SWA type 6 (dense cirrus). The middle layer of water clouds observed in the range of 37-39° N are considered to correspond to SWA type 6 (water cloud) and HCAI type 5 (middle cloud). In addition, since stratocumulus clouds are known as water clouds observed in the lower layer (Spinhirne, 1989), a lower layer of water clouds observed in the range of 35-36° N represent HCAI type 7 (stratocumulus). The ground-based data shown in Figures 7 and 8 indicate the possible existence of thin clouds over the Chiba area.

The cloud classification based on SWA13-15 shows that it detects more cloud types as compared with SWA15-16, but the classification based on SWA15-16 combination is useful for detecting cumulonimbus and middle cloud underneath dense cirrus regions. The HCAI method uses a number of bands, and hence, its implementation is often time consuming: besides, the accuracy of the resulting classification is not necessarily high since it uses the lapse rate for the retrieval of altitude information.

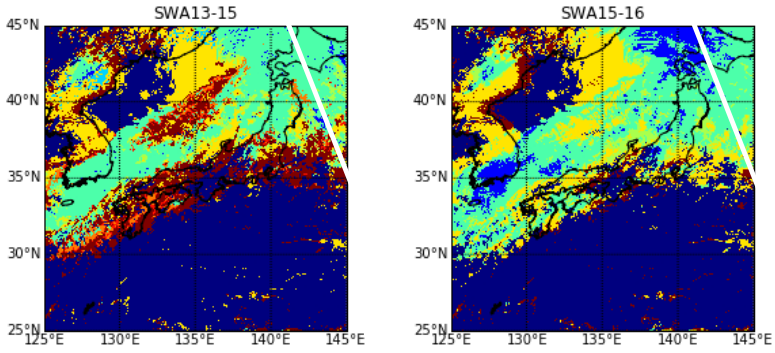

Type	SWA	HCAI
0	Clear	Clear
1	High Cb	Cu
2	Middle Cb	Dense Cloud
3	Cu	Cc
4	Dense Ci	Ci
5	ice Cloud	Middle Cloud
6	Water Cloud	Cu
7	Thick Ci	Sc
8	Cirrus	St
9	Thin Ci	No data

(a) SWA13-15 (b) SWA15-16 (c) Color bar

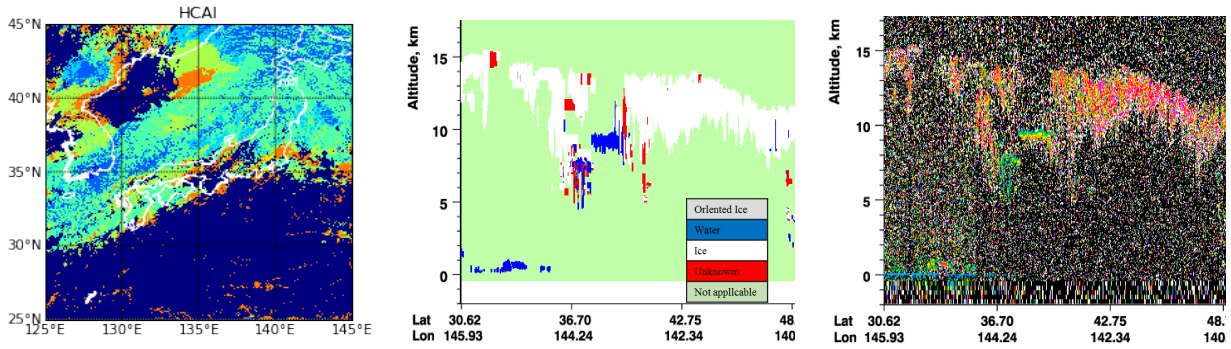

(d) HCAI (e) Cloud component (f) Depolarization ratio

Figure 6 Cloud analysis at 03:40 UTC on July 2, 2016

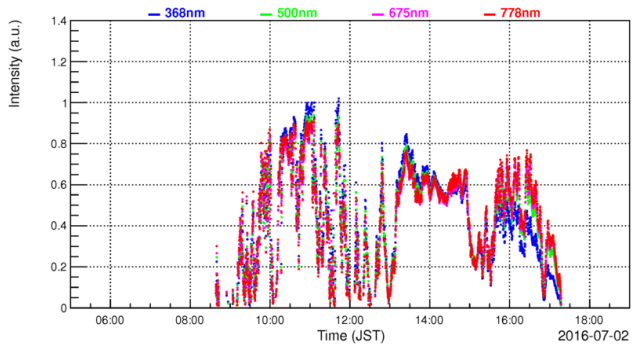

Figure 7 Intensity of sunphotometer signals on July 2, 2016.

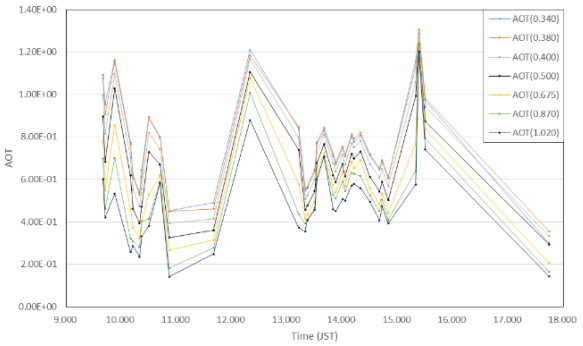

Figure 8 AOT on July 2, 2016

4 Conclusion

Comparison of two types of cloud classification methods (HCAI and SWA) has been implemented on Himawari data over the Japan area. The strengths and weaknesses in both classification methods have been examined and discussed. Because of its simplicity, the SWA approaches based on the band combinations of 13 -15 and 15 – 16 are useful for near real-time analysis of Himawari-8 data. The use of CALIPSO data as well as ground-based observation data can give more information about the cloud optical characteristics that can be used to improve the accuracy of the classification. In the future, more long-term analysis of clouds and aerosols will be undertaken from both satellite and ground-based measurements over the Chiba area.

References

1- Charles, R., 2019. NATIONAL AERONAUTICS AND SPACE ADMINISTRATION, Retrieved Aug 31, 2019, from https://www-calipso.larc.nasa.gov/

2- Higuchi, A., Takenaka, H., Toyoshima, K., 2018. Release note of "HIMAWARI 8" gridded data for full-disk (FD) observation mode, Retrieved Aug 31, 2019, from http://www.cr.chiba-u.jp/databases/GEO/H8_9/FD/index_jp.html

3- Jamrud, A., Okude, S., Lagrosas, N., Manago, N., Kuze, H., 2018. Real Time Derivation of Atmospheric Aerosol Optical Properties by Concurrent Measurements of Optical and Sampling Instruments, Open Journal of Air Pollution,7, pp141-145

4- Kuze, H., 2019. ADCL Ground Measurement Instruments, Retrieved Aug 31, 2019, from http://www.cr.chiba-u.jp/~kuze-lab/monitor/adcl.php

5- Mouri, K., Izumi, T., Shizue, H., Yoshida, R., 2016. Algorithm Theoretical Basis Document for Type/Phase Product, Meteorological satellite center technical note, 61, pp. 22-25

6- Murata, T., 2016. NICT Science Cloud, Retrieved Aug 31, 2019, from https://sc-web.nict.go.jp/himawari/

7- Purbantoro, B., Jamrud, A., Manago, N., Toyoshima, K., Lagrosas, N., Josaphat, T., Kuze, H., 2018. Comparison of Cloud Type Classification with Split Window Algorithm Based on Different Infrared Band Combinations of Himawari-8 Satellite, Advances in Remote Sensing, 7(3), pp218-234

8- Rajendra, K., Leo, M., 2014. Climate Change 2014: Synthesis Report, IPCC, Switzerland, pp2-26

9- Spinhirne, J., Boers, R., Hart, W., 1989. Cloud Top Water from Lidar Observations of Marine Stratocumulus, Journal of applied meteorology, 28, pp81

10- Stefanie, K., Larry, W., Marc, H., Markus, H., Terry, D,, Claudia, T., Matthew, T., Andrea, S., Joshua, P., Ralf, W., Stephan, F., Fred, J., Jean, P., Hans, S., John, E., Juan, C., Duncan, F., Mathias, P., Emmanuel, M., Justus, N., Markus, R., Christine, B., Filip, V., Adam, B., John, M., Daniel, K., Simon, A., Lieven, C., Thomas, T., Ryan, N., Alexander, D., Landon, R., James, C., Brian, M., 2016. Stratospheric aerosol-Observations, processes, and impact on climate, Reviews of Geophysics,54(2), pp278-280

11- Suzue, H., Imai, T., Mouri, K., 2016. High-resolution Cloud Analysis Information derived from Himawari-8 data, Meteorological satellite center technical note, 61, pp. 46-51